

Contents lists available at [SciVerse ScienceDirect](http://www.sciencedirect.com)

## Cancer Letters

journal homepage: [www.elsevier.com/locate/canlet](http://www.elsevier.com/locate/canlet)

## Original Articles

## Detection of a long non-coding RNA (CCAT1) in living cells and human adenocarcinoma of colon tissues using FIT–PNA molecular beacons

Yossi Kam<sup>a</sup>, Abraham Rubinstein<sup>a,b</sup>, Shankar Naik<sup>a</sup>, Irena Djavsarov<sup>a</sup>, David Halle<sup>c</sup>, Ilana Ariel<sup>d</sup>, Ali O. Gure<sup>e</sup>, Alexander Stojadinovic<sup>f</sup>, HongGuang Pan<sup>f</sup>, Victoria Tsvin<sup>c</sup>, Aviram Nissan<sup>c,\*</sup>, Eylon Yavin<sup>a,\*</sup>

<sup>a</sup>The Hebrew University of Jerusalem, Faculty of Medicine, The School of Pharmacy, Institute for Drug Research, P.O. Box 12065, Jerusalem 91120, Israel

<sup>b</sup>The Harvey M. Krueger Family Center for Nanoscience and Nanotechnology and the David R. Bloom Center of Pharmacy of the Hebrew University of Jerusalem, Israel

<sup>c</sup>Department of Surgery, Hadassah-Hebrew University Medical Center, Ein Kerem, P.O. Box 12000, Jerusalem 91120, Israel

<sup>d</sup>Department of Pathology, Hadassah-Hebrew University Medical Center, Mount Scopus, P.O. Box 24035, Jerusalem 91240, Israel

<sup>e</sup>Department of Molecular Biology and Genetics, SB-248 Bilkent University Ankara, Turkey

<sup>f</sup>Department of Surgery, Walter Reed National Military Medical Center, Bethesda, MD, USA

## ARTICLE INFO

## Article history:

Received 3 January 2013

Received in revised form 6 February 2013

Accepted 6 February 2013

Available online xxx

## Keywords:

Colorectal cancer  
Molecular beacon  
Peptide nucleic acid  
Long non-coding RNA  
Imaging

## ABSTRACT

Although the function and mechanism of action of long non-coding RNAs (lncRNA) is still not completely known, studies have shown their potential role in the control of gene expression and regulation, in cellular proliferation and invasiveness at the transcriptional level via multiple mechanisms. Recently, colon cancer associated transcript 1 (CCAT1) lncRNA was found to be expressed in colorectal cancer (CRC) tumors but not in normal tissue. This study aimed to study the ability of a CCAT1-specific peptide nucleic acid (PNA) based molecular beacons (TO-PNA-MB) to serve as a diagnostic probe for *in vitro*, *ex vivo*, and *in situ* (human colon biopsies) detection of CRC. The data showed enhanced fluorescence upon *in vitro* hybridization to RNA extracted from CCAT1 expressing cells (HT-29, SW-480) compared to control cells (SK-Mel-2). Uptake of TO-PNA-MBs into cells was achieved by covalently attaching cell penetrating peptides (CPPs) to the TO-PNA-MB probes. *In situ* hybridization of selected TO-PNA-MB in human CRC specimens was shown to detect CCAT1 expression in all (4/4) subjects with pre-cancerous adenomas, and in all (8/8) patients with invasive adenocarcinoma (penetrating the bowel wall) tumors. The results showed that CCAT1 TO-PNA-MB is a powerful diagnostic tool for the specific identification of CRC, suggesting that with the aid of an appropriate pharmaceutical vehicle, real time *in vivo* imaging is feasible. TO-PNA-MB may enable identifying occult metastatic disease during surgery, or differentiating in real time *in vivo* imaging, between benign and malignant lesions.

© 2013 Elsevier Ireland Ltd. All rights reserved.

## 1. Introduction

Colorectal cancer (CRC) is a common disease with over a million new cases diagnosed annually worldwide. In developed countries, most CRC cases are diagnosed in early stage while treatment with curative intent is still feasible. However, even in developed countries, about a quarter of CRC cases are diagnosed at a relatively late stage, when it has already spread and distant metastasis appear

[1]. Some patients with metastatic disease are treated with curative intent. However, even the combination of best available systemic agents with radical surgery offers long-term survival to only 30% of CRC patients treated in the metastatic stage of the disease. One possible explanation for the high recurrence rate is occult tumor deposits resistant to chemotherapy left untreated because they are too small to be viewed by the naked eye. A real-time *in vivo* imaging that would target such occult lesions could improve the surgeon's ability to detect and remove those deposits, thus improving the medical outcome. In the past, radio-immuno guided surgery (RIGS) was attempted [2] unsuccessfully due to the lack of suitable markers, high background signal, and radiation.

Colon cancer progression is highly dependent on the accumulation of gene alternations. Fearon and Vogelstein were the first to suggest the “adenoma–carcinoma” multistep model [3], that begins with the loss of APC, the tumor suppressor gene responsible

**Abbreviations:** CCAT1, colon cancer associated transcript-1; CRC, colorectal cancer; CPP, cell penetrating peptide; TD-CPP, transdermal cell penetrating peptide; FISH, fluorescence *in situ* hybridization; PNA, peptide nucleic acid; MB, molecular beacon; PFI, pure fluorescence intensity; lncRNA, long non-coding RNA; TO, thiazole orange.

\* Corresponding authors. Tel.: +972 2 6778800; fax: +972 2 6449412 (A. Nissan), tel.: +972 2 6758692; fax: +972 2 6757076 (E. Yavin).

E-mail addresses: [anissan@hadassah.org.il](mailto:anissan@hadassah.org.il) (A. Nissan), [eylon@ekmd.huji.ac.il](mailto:eylon@ekmd.huji.ac.il) (E. Yavin).

0304-3835/\$ - see front matter © 2013 Elsevier Ireland Ltd. All rights reserved.  
<http://dx.doi.org/10.1016/j.canlet.2013.02.014>

Please cite this article in press as: Y. Kam et al., Detection of a long non-coding RNA (CCAT1) in living cells and human adenocarcinoma of colon tissues using FIT–PNA molecular beacons, *Cancer Lett.* (2013), <http://dx.doi.org/10.1016/j.canlet.2013.02.014>

for preventing mucosal hyperproliferation [4], followed by mutations of the genes DCC [3], MCC [5], ras [6], and P53 [7]. Some genes may lose function (APC, DCC, p53), while some oncogenes (KRAS, BRAF) may gain function. Since then, several other molecular pathways leading to the phenotype known as CRC were discovered [8–10].

Non-coding RNAs play a significant role in the control of gene expression and regulation and their function in tumorigenesis received much attention over the past decade [11–13]. Small interference RNA (siRNA) and microRNA (miRNA) were extensively studied and shown to be essential regulators of various processes such as proliferation, differentiation, development, and cell death [14–17]. Quantification and imaging of miRNA were also reported [18,19]. For other non-coding RNAs, such as long non-coding RNAs (lncRNAs), the function and mechanism of action is yet to be elucidated. Recent studies indicate the potential role of lncRNAs in cellular proliferation and invasion [13,20–23]. Some lncRNA were shown to be overexpressed in cancerous tissue and in cancer cell lines [24] and some were strongly correlated with poor patient prognosis and metastasis [25–29].

Recently, Nissan and coworkers have identified a lncRNA transcript, colon cancer associated transcript-1 (CCAT1), highly expressed in CRC but not in normal tissues. Because CCAT1 is upregulated in the vast majority of primary CRC tumors, in precancerous polyps (adenomas), lymph nodes, blood, and distant CRC metastasis [30], it may serve as an efficient target for real-time *in vivo* imaging.

In a previous study [31] we showed that endogenous mutant K-ras mRNA could be hybridized and detected in living (un-fixed) cancer cells by MBs [32]. We also showed that more stable MB, based on peptide nucleic acid (PNA), containing a surrogate base (known as forced intercalation (FIT)) that served as a light-up probe [33–36], could discriminate the mutated K-ras mRNA transcript at a single base resolution. In the present study we show that a well designed PNA molecular beacon (PNA-MB) complementary to lncRNA-CCAT1 can be used as a tool for imaging cell lines and detecting malignancies in human CRC biopsies *in situ*.

## 2. Materials and methods

All materials were purchased from Sigma–Aldrich, (St. Louis, MO, USA), unless otherwise stated. All solvents were analytical grade. Water was purified by reverse osmosis.

### 2.1. Cell lines and their culturing

SW-480 and HT-29 (human colon adenocarcinoma) cells, both expressing the lncRNA CCAT1 sequence and SK-Mel-2 melanoma cell line that does not express the lncRNA CCAT1, were purchased from the American Type Culture Collection (ATCC, Manassas, VA, USA). HT29 and SW-480 cells were cultured (37 °C, 5% CO<sub>2</sub>) in DMEM medium supplemented with 10% fetal calf serum, 2 mM L-glutamine, and 100 mg/ml streptomycin (Beit Haemek Biological Industries, Beit Haemek, Israel). SK-Mel-2 cells were cultured in EMEM medium supplemented with 10% fetal calf serum, 2 mM L-glutamine, and 100 mg/ml streptomycin.

### 2.2. Molecular beacons – design and synthesis

The sequences of the thiazole orange-peptide nucleic acid molecular beacons (TO-PNA-MB) were designed using the m-fold program (UNAFold, a unified nucleic acid folding and hybridization simulation package, RNA Institute, Albany, NY, USA) targeting different sites along the CCAT1 sequence [37]. The specificity of the selected sequences was examined using BLAST analysis. Complementary DNA probes were synthesized by Integrated DNA Technologies (IDT, Iowa, USA). All target DNA sequences were 50 bases long (Table 1).

### 2.3. Synthesis of CPP TO-PNA-MB

PNA synthesis was performed using Fmoc solid-phase synthesis on Fmoc-Lys (Boc)-Novasyn-TGA resin as previously described [38]. The PNA-TO monomer was synthesized as described previously [31,36,39] with the exception of increasing the temperature during TO-CH<sub>2</sub>COOH coupling to the PNA backbone to 55 °C

**Table 1**

The complementary CCAT1 DNA sequence used as targets for the TO-PNA-MB. Hybridization sites are underlined.

Target site on CCAT1	Complementary DNA sequence
180–194	ACC TGG CCA GCC CTG <u>CCA CTT ACC AGG TTG GCT</u> CTG TAT GGC TAA GCG TT
565–581	GAT AAC TAG AGA <u>ATC ACC CAA TCT ACT CCC</u> ATT TTC AAC TCT AAA TCA TC

(DMF, 5 h) in order to improve yields. To allow cell transfection of the TO-PNA-MB, cell penetrating peptides (CPPs) were synthesized on the C-terminus of the TO-PNA-MB.

Two types of CPP were examined: 8 L-lysines or *transdermal peptide* (TD) [26] (Table 2). Two lysine residues were also added at the N-terminus of the TO-PNAs mainly to improve TD-TO-PNA-MB water solubility. Cleavage of the final PNA product from the solid support was performed in trifluoroacetic acid and m-cresol (95%:5%). Diethyl-ether was added and the precipitate was collected, dissolved in water, frozen, and lyophilized. PNA was purified and analyzed by HPLC (Shimadzu LC-1090, Shimadzu Corporation, Tokyo, Japan) on a semi-preparative C18 reverse-phase column (Jupiter 300 A, Phenomenex, Torrance, CA, USA) using acetonitrile and 0.1% TFA in water as eluents. TO-PNA-MB purity was verified by mass analysis (MALDI-TOF MS, Voyager De Pro, Applied Biosystems, CA, USA) and found to be >90% pure. PNA sample concentration was calculated using a Nanodrop® Spectrophotometer (Nanodrop Inc., Wilmington, DE, USA) at 260 nm.

### 2.4. In vitro hybridization analysis with synthetic constructs

TO-PNA-MBs were tested *in vitro* for their ability to hybridize to 50 base long synthetic DNA targets (Table 1) by incubating (60 min, 37 °C) 50 nM of each MB probe with 100 nM of the target sequences in a 96-well plate. The incubation was carried out in hybridization buffer (20 mM Tris-HCl, 50 mM KCl, 10 mM MgCl<sub>2</sub>, pH = 8). Fluorescence intensity of each well was measured ( $\lambda_{\text{EX}}$ : 485 nm;  $\lambda_{\text{EM}}$ : 521 nm) by a microplate reader (Synergy HT Multi-Mode, Bio-tek, VT, USA). Measured fluorescence was compared to the fluorescence obtained from TO-PNA-MB probe without a DNA target.

### 2.5. Quantitative reverse-transcriptase polymerase chain reaction (qRT-PCR)

One microgram of total RNA extracted from different cell lines was used for reverse transcription with random primers in a 20  $\mu$ l reaction of which 2  $\mu$ l was used for polymerase chain reaction (PCR). All experiments were conducted in duplicates. qRT-PCR was performed for 40 cycles (denaturation: 95 °C  $\times$  15 s; annealing/extension: 60 °C  $\times$  1 min) with the primers and TaqMan® probe specific for human GAPD (GAPDH). The GAPDH endogenous control (VIC/MGB Probe, Primer Limited, 4326317E) was obtained from Applied Biosystems, Foster City, CA, USA.

For CCAT1 expression analysis, the primers and probe used were custom-made using the GeneBank sequence HM358356 as follows:

- Forward primer: 5'-TCACTGACAACATCGACTTTGAAG.
- Reverse primer: 5'-GGAGAAAACGCTTAGCCATACAG.
- Probe: 6Fam-CTGGCCAGCCCTGCCACTTACCA-Tamra.

Relative quantification was done according to the manufacturer's instructions (Applied Biosystems, Foster City, CA, USA; User Manual 2). Each sample was normalized according to its GAPDH content and also against a calibrator set constructed of RNA obtained from normal colon tissue (AmbionVR Austin, TX, USA). The relative quantity (RQ) was determined according to the ddCT method using the following equation:

$$RQ = 2^{(\Delta\text{CT}_{\text{CCAT1}} - \Delta\text{CT}_{\text{GAPDH}})} \quad (1)$$

All experiments were performed using an ABI Prism 7500 system (Applied Biosystems, Foster City, CA, USA).

### 2.6. In vitro hybridization assay with total RNA

RNA was isolated from the cells by using an RNA isolation kit (TRI Reagent®, Molecular Research Center, Inc. Cincinnati, OH, USA) according to the manufacture instructed protocol. CPP-TO-PNA-MBs were incubated with 1  $\mu$ g total RNA isolated from cells that express the lncRNA-CCAT1 (SW-480 or HT-29) and non expressing cells (SK-Mel-2). One microgram of the extracted RNA was incubated (60 min, 50 °C followed by 1 h at room temperature) with 100 nM of the TO-PNA-MBs. The resulted fluorescence defined as crude fluorescence value (CFV) was monitored ( $\lambda_{\text{EX}}$ : 485 nm;  $\lambda_{\text{EM}}$ : 521 nm) in a microplate reader (Synergy HT Multi-Mode, Biotek, VT, USA).

**Table 2**  
The CPP-TO-PNA-MB sequences and their Mw characterization.

CPP-PNA product	CPP-PNA-sequence	Calculated Mw	Found Mw
K8-180 <sup>a</sup>	K(8)-CCAACT-TO-GTAAGTG-KK	5510.0	5517.9
TD-180 <sup>a</sup>	ACSSSPSKHCG-CCAACT-TO-GTAAGTG-KK	5559.6	5586.7
K8-564 <sup>a</sup>	K(8)-TAGTGG-TO-TTAGATGAGG	5958.0	5953.0

<sup>a</sup> Location on the CCAT1 transcript.

In hybridization experiments, the fluorescence of the PNA probes in hybridization buffer and in the absence of target was defined as the pure fluorescence value (PFV). This value was subtracted from CFV and this difference was defined as the pure fluorescence intensity (PFI).

### 2.7. Cellular uptake analysis

Forty-eight hours prior to hybridization, SW-480, HT-29, and SK-Mel-2 cells were plated separately, on chamber slides (Ibidi GmbH, Munich, Germany) until reaching 70–80% confluence. Cells were washed with serum free medium approximately 1 h before the TO-PNA-MB was added to each well.

#### 2.7.1. Hybridization and imaging in living cells

The cells were incubated (24 h, 37 °C, humidified atmosphere containing 5% CO<sub>2</sub>), with 500 nM of the TO-PNA-MB in complete medium. 24 h later, the medium was replaced; cells were washed with PBS (3×) and imaged by confocal microscopy.

### 2.8. In situ hybridization

Human specimen collection was performed according to a previously described protocol [30]. Briefly, patients over the age of 18 years with histologically confirmed primary adenocarcinoma or adenoma of the colon were offered participation in the study. Patients who received prior radiation or chemotherapy were excluded from the study. The study protocol was approved by the Institutional Review Board (IRB, Helsinki Committee) of Hadassah-Hebrew University Medical Center. All specimens were submitted for standard histopathological examination. Formalin-fixed paraffin-embedded samples were stained with hematoxylin and eosin (H&E). Patients meeting eligibility criteria ( $n = 12$ ) signed an IRB-approved informed consent and were enrolled into the study. There were patients with adenoma ( $n = 4$ ) and patients with invasive adenocarcinoma ( $n = 8$ ).

### 2.9. Fluorescence in situ hybridization (FISH) of the human colon specimens

#### 2.9.1. Tissue preparation

Five micron thick paraffin-embedded specimens were de-paraffinized by melting (hot plate, 45 °C, 30 min) and rinsed with xylene (2×, RT, 10 min). Xylene was then removed by soaking the slides in absolute ethanol (2×, RT, 10 min). The slides were then dried in air (5 min), digested with pepsin (5 mg/ml in 0.85% NaCl, pH = 1.5, 7 min, 45°C) following by two consecutive washes (1 min) with fresh saline-sodium citrate buffer (0.30 M sodium citrate/0.030 M NaCl in 100 ml, pH = 7). Acetylation (to reduce probe electrostatic binding to positively charged regions on the tissues as a means of reducing tissue background fluorescence) was performed by stirring the pre-treated (triethanolamine, 0.1 M, pH = 8) slides with 0.25% v/v of acetic anhydride (RT, 10 min). After a second wash with PBS and saline-sodium citrate (0.15 M sodium citrate, 0.015 M NaCl in 100 ml, pH = 7), the slides were dehydrated with elevated concentrations of ethanol and air dried.

#### 2.9.2. Hybridization

Hybridization was conducted with the 180-TO-PNA-MB probe by its incubation (500 nM) with each of the slides, after sealing with a cover slip and a rubber cement. The slides were then placed on a hot plate (80 °C, 90 s), followed by hybridization in a self-made humidified chamber to allow hybridization (RT, 1 h). The rubber cement was then carefully removed and the unbound 180-TO-PNA-MB was removed by washing with 70% formamide/10 mM Tris-HCl (pH = 7)/0.1%BSA (2×, RT, 15 min each) followed by 5 min consecutive washes in 0.1 M TRIS-HCl (pH = 7)/0.15 M NaCl/0.08% Tween 80. Dehydration was conducted with elevated concentrations of ethanol and air dried. Mounting media (Fluoromount<sup>®</sup>) was then applied on the slides, covered with coverslip and imaged by confocal microscopy (Olympus, FV300 laser scanning confocal, Japan).

#### 2.9.3. Image analysis

The preferential binding fluorescent intensity of the 180-TO-PNA-MB probe to tissue specimens was quantified by the spectral analysis ASI computer program (Applied Scientific Instrumentation, Eugene, Oregon, USA). The program converts the signal intensity per pixel to a scalable intensity that is then presented as relative intensity on a color scale bar.

## 3. Results

### 3.1. TO-PNA-MB: design and hybridization properties

To optimize the TO-PNA-MB ability to bind the lncRNA CCAT1, two PNAs were designed, synthesized, and tested for their hybridization capabilities (see experimental Sections 2.2–2.3 for details).

### 3.2. Hybridization with synthetic DNA

In order to select the best TO-PNA-MB, the magnitude of the *in vitro* hybridization of 565-581 TO-PNA-MB and 180-194 TO-PNA-MB with the complementary synthetic DNA target sequences was studied. The results shown in Fig. 1, which also presents the internal fluorescence of each TO-PNA-MB, indicate a 6-fold signal-to-background ratio, regardless of PNA sequence.

### 3.3. lncRNA CCAT1 quantification in total RNA extracts

lncRNA CCAT1 expression in total RNA extracts from SW-480, HT-29, and SK-Mel-2 cells, and commercial normal colon tissue RNA was quantified by qRT-PCR. The relative quantification (RQ) of CCAT1 expression in SW-480 and HT-29 cells was significantly higher compared to its expression in the SK-Mel-2 cells and in the normal colon control as shown in Table 3. These results validate the published data of CCAT1 in the studied cell lines [30].

### 3.4. Hybridization with total RNA

RNA extracted from the different cell lines (HT-29, SW-480, and SK-Mel-2) was incubated with the two TO-PNA-MBs in order to study the increase in fluorescence due to specific hybridization. The pure fluorescence intensity (PFI) was calculated by subtracting the background fluorescence measured from TO-PNA-MB in hybridization buffer only (defined as pure fluorescence value (PFV)) from the fluorescence of TO-PNA-MB in crude RNA cell extract (defined as crude fluorescence value (CFV)). The PFI of the two CCAT1-targeting TO-PNA-MBs is shown in Fig. 2. In order to study the increase in CFV as a result of TO-PNA-MB hybridization,

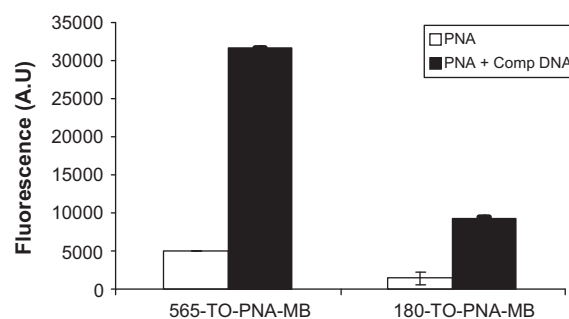


**Fig. 1.** The signal to background ratio of two CCAT1-targeting TO-PNA-MBs. Background fluorescence (empty columns) and hybridization-derived fluorescence (filled columns) of 565-TO-PNA-MB (left) and 180-TO-PNA-MB (right). Shown are the mean values of 3 different experiments  $\pm$  S.D.

**Table 3**  
Validation of CCAT1 expression in cell lines used for the study.

Specimen (known CCAT1 expression)	Relative quantification
Normal colon tissue (CCAT1 low)	1.0
HT-29 cells (CCAT1 high)	172,195.5
SW-480 cells (CCAT1 high)	27,304.2
SK-Mel-2 cells (CCAT1 negative)	<1.0

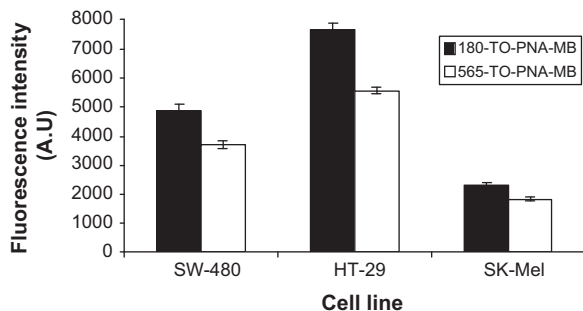


**Fig. 2.** The pure fluorescence intensity (PFI, in arbitrary units) caused by hybridizing 180-TO-PNA-MB (filled columns) or 565-TO-PNA-MB (empty columns) to total RNA extracted from HT-29 and SW-480 (highly expressing CCAT1) and SK-Mel-2 (CCAT1 negative control) cells. Shown are the mean values of 3 different experiments  $\pm$  S.D.

the CFV of expressing cells was divided by the PFI of the non-expressing cells (SK-Mel-2). PFI was found to be 4-fold higher in HT-29 and 2-fold higher in SW-480 regardless of TO-PNA-MB sequence reflecting the relative quantity of CCAT1 expression in each cell line.

### 3.5. TO-PNA-MB hybridization in living cells

Prior to the hybridization studies, the capability of the CPPs K8 and TD to transfect the tested cells with the appropriate TO-PNA-MB was studied.

Cells were incubated with either TD-180-TO-PNA-MB or K8-180-TO-PNA-MB, washed and imaged by confocal microscopy. There was no fluorescence detected with hybridization to SK-Mel cells. As demonstrated in Fig. 3, in both HT29 and SW480 cells, the K8-180-TO-PNA-MB showed a superior cellular uptake compared to the TD-180-TO-PNA-MB. We therefore pursued our studies using K8 as a CPP. In terms of sequence specificity, both TO-PNA-MB sequences were able to discriminate the lncRNA CCAT1 expressing cells, HT-29 and SW-480 from the CCAT1 negative SK-Mel-2 cells, with slightly higher fluorescence intensity for the K8-180-TO-PNA-MB compared to the K8-565-TO-PNA-MB (Fig. 4). These observations support the results shown in Fig. 2 (hybridization with total RNA extracts) where fluorescence ratios using the 180-TO-PNA-MB were slightly higher than those of 565-TO-PNA-MB.

### 3.6. FISH in human colonic tissues

The next step was to show specific staining of adenoma and adenocarcinoma human tissues. FISH staining was performed using the 180-TO-PNA-MB that was shown to bind specifically to the target RNA in cell culture. Detection of lncRNA-CCAT1 was conducted on paraffin-embedded human tissues. Representative tissues of adenoma, adenocarcinoma, and normal colonic mucosa were selected and the correct diagnosis was verified pathologically using H&E stained slides.

FISH staining was conducted on matched “normal-adenocarcinoma” and “normal-adenoma” from the same patient. The

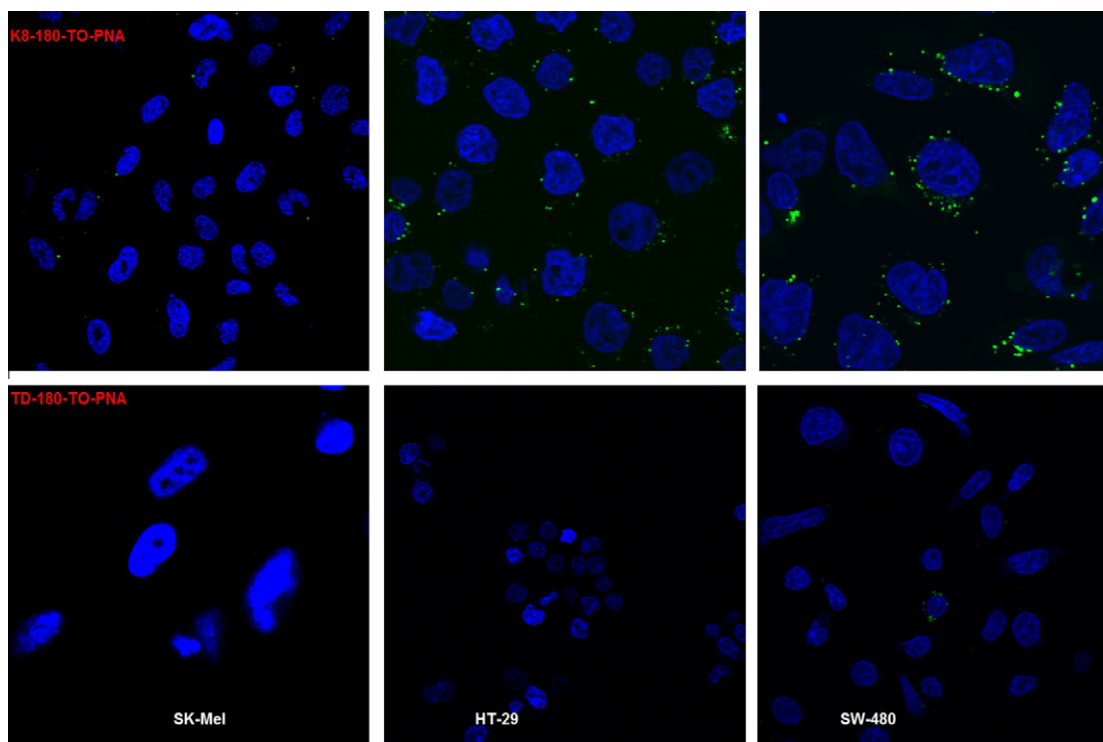


**Fig. 3.** Confocal laser scanning microscopy images (60 $\times$ ) of HT-29, SW-480, and SK-Mel-2 cells following 24 h incubation with K8-180 TO-PNA-MB and TD-180 TO-PNA-MB. Green: TO fluorescence ( $\lambda_{\text{ex}}$ : 488 nm) is clearly seen in the upper panel (internalization of the 180-TO-PNA-MB with the 8 lysines) indicating successful cell-internalization and hybridization with the lncRNA CCAT1. Blue: nuclear staining with Hoechst reagent ( $\lambda_{\text{ex}}$ : 350 nm) which was conducted to delineate cells' orientation. (For interpretation of the references to color in this figure legend, the reader is referred to the web version of this article.)

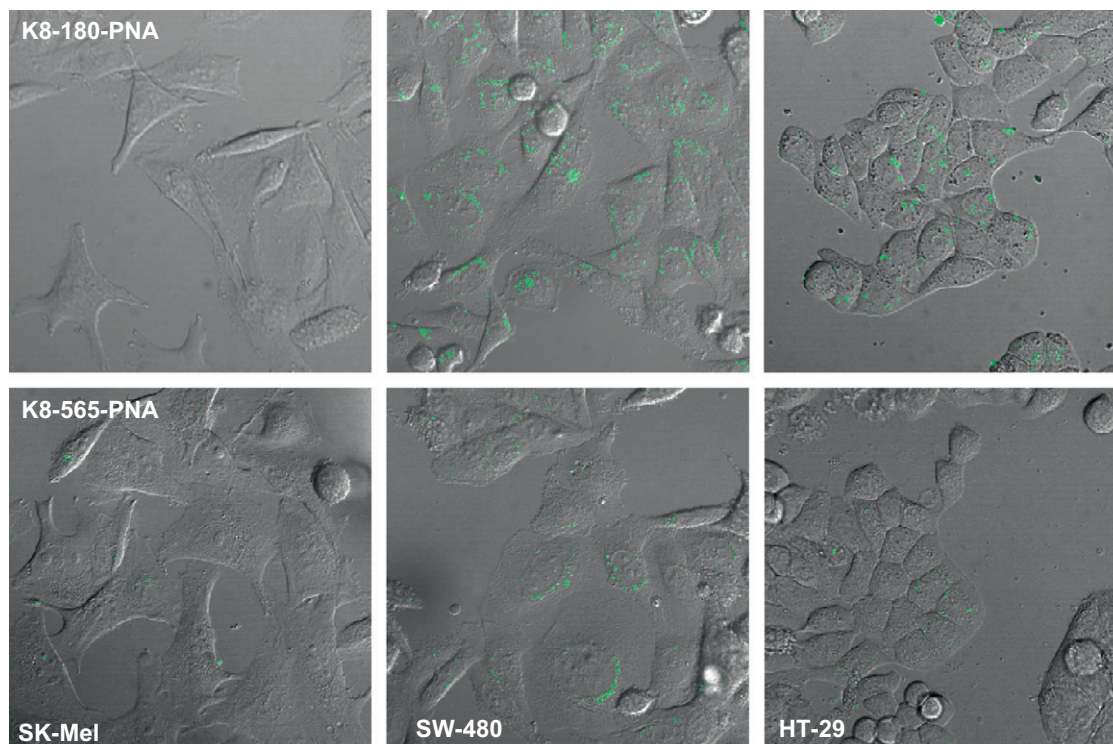


**Fig. 4.** Confocal microscopy images (60 $\times$ ) of SK-Mel-2 (control), SW-480 m, and HT-29 cells, following 24 h incubation with K8-180-TO-PNA or K8-565-TO-PNA. Green: TO fluorescence, indicating successful hybridization of the PNA-CCAT1 with cellular lncRNA with a slight advantage of the K8-180-TO-PNA-MB over the K8-565-TO-PNA-MB. (For interpretation of the references to color in this figure legend, the reader is referred to the web version of this article.)

CCAT1-specific 180-TO-PNA-MB showed significantly higher fluorescence intensity in the adenoma and adenocarcinoma tissues compared with their matched normal colon tissues, reflecting specific and uniform binding of the 180-TO-PNA-MB to CCAT1 expressing human tissues (Fig. 5). Fluorescence was observed at the luminal aspect of the colonic mucosa, especially in the crypts regions.

#### 4. Discussion

The ability to detect occult metastatic disease at the time of surgery and the ability to differentiate benign from malignant tissues may improve the outcome of oncological surgery and may reduce recurrence rate. The conjugation of radio-isotopes to antibodies directed against cancer-specific antigens such as carcinoembryonic antigen (CEA) or tumor-associated glycoprotein 72 (TAG72) was studied by many and even entered clinical practice in the form of the CEA-scan or RIGS. However, this real-time *in vivo* imaging method was abandoned mainly because of the high background to signal ratio, non-specific readings together with the radiation hazard [40–43]. In order to overcome these obstacles, we drafted a platform that will enable the surgeon to detect occult metastasis with high accuracy and without radiation exposure. Our previous study [31] showed that PNA-MB directed to K-ras mutations was able to differentiate cells containing K-ras mutations from cells with wild-type K-ras. Since our long-term goal is to detect a wide range of colonic neoplasms we decided to further design PNA-MBs directed not only to somatic mutations but also to intra-cellular transcripts upregulated in adenomas and adenocarcinomas of the colon, such as long non-coding RNAs. The lncRNA, CCAT1 [30], upregulated in adenomas and adenocarcinomas of the colon in all stages was selected as a target. Verifying CCAT1 expression in the cell lines used in this study enabled us to proceed to examine living cells. This was conducted by simple incubation of CPP-PNA-

TO-MBs with the relevant cells [44]. Both K8-565-TO-PNA-MB and K8-180-TO-PNA-MB were able to generate hybridization in the CCAT1 expressing cells, HT29 and SW480. Negligible fluorescence was detected in the CCAT1 SK-Mel-2 cells (negative control). We also considered another control experiment which was the CCAT-1 expressing cell line (HT29) that was treated with siRNA designed to silence this lncRNA (see supporting information). The idea was to add the PNA probes to such a cell line and follow an expected decrease in fluorescence. Although CCAT-1 levels were substantially reduced after cell transfection, the viability of these cells was significantly low (as measured by MTT assay). Therefore we did not consider this approach as a valid one for diagnostic purposes.

To the best of our knowledge, this is the first report describing the use of PNA-MB for detecting lncRNAs in living cells and in human biopsies. This highlights the potential of such probes in detecting a variety of RNA species such as mRNA [31], viral RNA [34], miRNA[45] and now, lncRNA.

Finally, the K8-180-TO-PNA-MB was tested for its competence to generate *in situ* hybridization and specific fluorescence in human colon normal, adenoma and adenocarcinoma tissues. PNA technology was tested before for *in situ* hybridization [46,47] showing the possible use of PNA probes for detecting HIV-1 viral DNA in cells or the possible use of PNA probes to detect specific RNA alternative splicing variants characterizing RNA isoforms at the subcellular level.

In our study, profound fluorescence was obtained in all stained adenomas and adenocarcinomas when incubated with K8-180-TO-PNA-MB, while incubation with normal tissues from the same patients resulted in much lower fluorescence that could be related to background noise. This observation corresponds to the PCR analysis published previously, that showed high CCAT1 expression in adenomas and carcinomas and low CCAT1 expression in normal colonic mucosa of the same patients [30]. This specific fluorescent

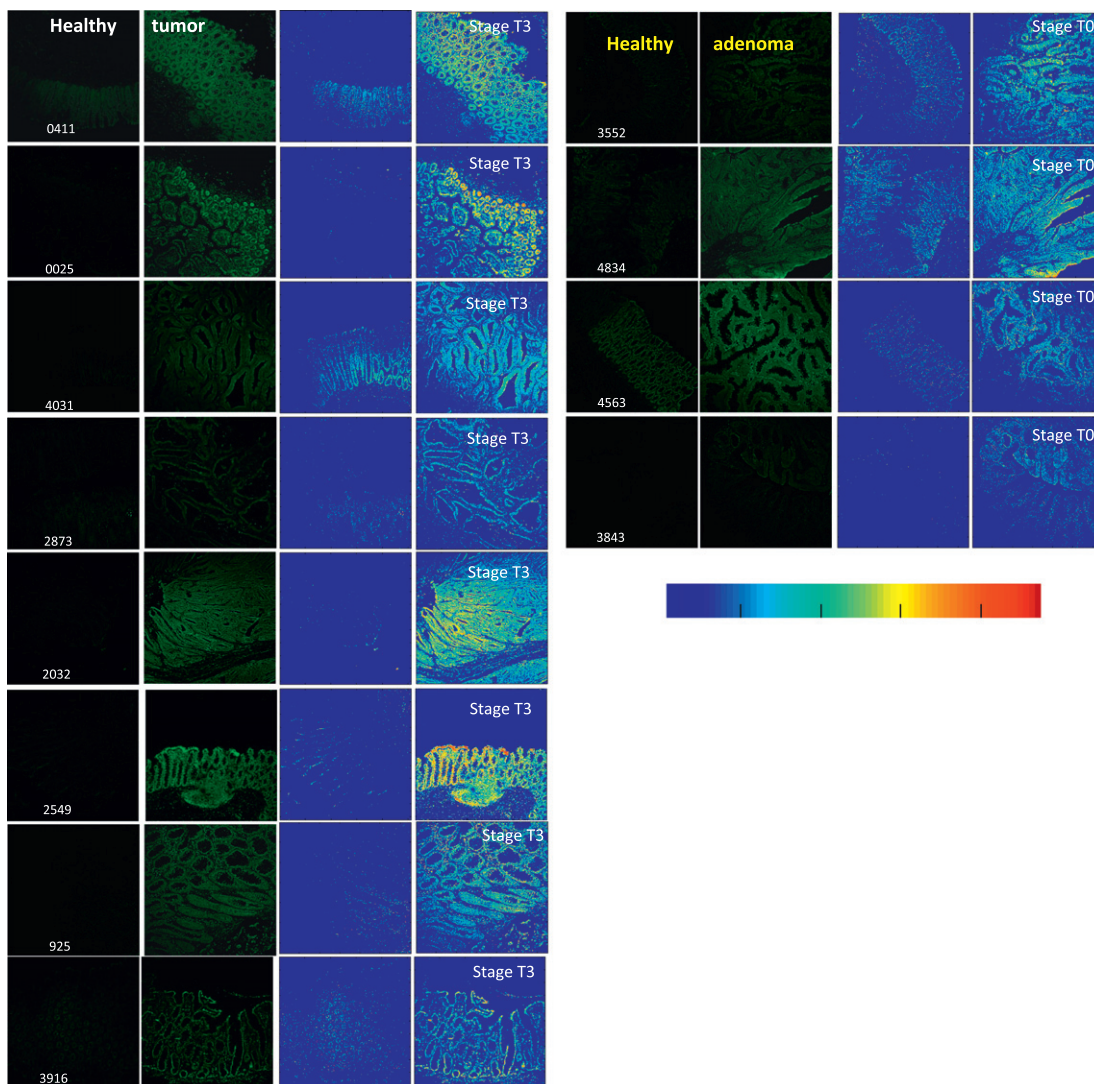


**Fig. 5.** FISH images of paraffin-embedded human colon tissues after incubation with 180-TO-PNA-MB. While the normal (“healthy”) tissues (left) show low (background) fluorescence, the tumor and adenoma specimens (right) show profoundly high fluorescence intensity. In the left two panels, images (10×) from each set of patients were taken by confocal laser scanning microscopy using a 488 nm laser (TO excitation). ASI image analysis of each specimen (right two blue panels) distinguishes even better between the healthy and the cancerous tissues. Stage T0 = American joint committee on Cancer (AJCC) T-stage (no invasive cancer); Stage T3 = AJCC T-stage (adenocarcinoma penetrating the bowel wall) as identified pathologically (H&E stain). (For interpretation of the references to color in this figure legend, the reader is referred to the web version of this article.)

signal in the adenoma tissue suggests that such PNA-MBs could potentially be used, clinically, for differentiation, in real time, between adenomas and benign polyps such as hyperplastic polyps or hamartomas. Such sensitivity would allow a fast and simple approach for processing biopsies taken from such lesions in order to establish a more reliable and sensitive diagnostic decision.

## 5. Conclusions

TO-PNA-based MBs were shown to elicit a specific fluorescence signal when hybridized to the specific lncRNA CCAT1 target in living cells and in human biopsies. This highlights the medical potential of using such PNAs for the detection and staging of CRC and as a supportive tool for the surgeon.

## Acknowledgements

The results reported here are included in the dissertation Project of Y.K. in partial fulfillment of his Ph.D. degree requirements

at The Hebrew University of Jerusalem. E.Y. acknowledges the David R. Bloom Center for Pharmacy and the Grass Center for Drug Design and Synthesis of Novel Therapeutics for financial support. A.R. acknowledges the Israel Cancer Association for financial support.

## Appendix A. Supplementary material

Supplementary data associated with this article can be found, in the online version, at <http://dx.doi.org/10.1016/j.canlet.2013.02.014>.

## References

- [1] A. Andriulli, S. Loperfido, G. Napolitano, G. Niro, M.R. Valvano, F. Spirito, A. Pilotto, R. Forlano, Incidence rates of post-ERCP complications: a systematic survey of prospective studies, *Am. J. Gastroenterol.* 102 (8) (2007) 1781–1788.
- [2] L. Mansi, E. Di Lieto, P.F. Rambaldi, C. Bergaminelli, F. Fallanca, G. Vicidomini, V. Cuccurullo, R. Mancusi, Preliminary experience with radioimmuno-guided surgery of primary neoplasms of the lung, *Minerva Chir.* 53 (5) (1998) 369–372.

- [3] E.R. Fearon, B. Vogelstein, A genetic model for colorectal tumorigenesis, *Cell* 61 (5) (1990) 759–767.
- [4] J. Groden, A. Thliveris, W. Samowitz, M. Carlson, L. Gelbert, H. Albertsen, G. Joslyn, J. Stevens, L. Spirio, M. Robertson, L. Sargeant, K. Krapcho, E. Wolff, R. Burt, J.P. Hughes, J. Warrington, J. McPherson, J. Wasmuth, D. Lepaslier, H. Abderrahim, D. Cohen, M. Leppert, R. White, Identification and characterization of the familial adenomatous polyposis coli gene, *Cell* 66 (3) (1991) 589–600.
- [5] K.W. Kinzler, M.C. Nilbert, B. Vogelstein, T.M. Bryan, D.B. Levy, K.J. Smith, A.C. Preisinger, S.R. Hamilton, P. Hedge, A. Markham, M. Carlson, G. Joslyn, J. Groden, R. White, Y. Miki, Y. Miyoshi, I. Nishisho, Y. Nakamura, Identification of a gene located at chromosome 5q21 that is mutated in colorectal cancers, *Science* 251 (4999) (1991) 1366–1370.
- [6] J.L. Bos, E.R. Fearon, S.R. Hamilton, M. Verlaan-de Vries, J.H. van Boom, A.J. van der Eb, B. Vogelstein, Prevalence of ras gene mutations in human colorectal cancers, *Nature* 327 (6120) (1987) 293–297.
- [7] M. Hollstein, D. Sidransky, B. Vogelstein, C.C. Harris, P53 mutations in human cancers, *Science* 253 (5015) (1991) 49–53.
- [8] L. Evangelista, M.C. Marzola, S. Chondrogiannis, A. Al-Nahhas, D. Rubello, Colorectal cancer: translation of biological pathways into molecular imaging, *Nucl. Med. Commun.* 33 (7) (2012) 780–782.
- [9] F.A. Sinicrope, D.J. Sargent, Molecular pathways: microsatellite instability in colorectal cancer: prognostic, predictive, and therapeutic implications, *Clin. Cancer Res.* 18 (6) (2012) 1506–1512.
- [10] S. Al-Sohaily, A. Biankin, R. Leong, M. Kohonen-Corish, J. Warusavitarne, Molecular pathways in colorectal cancer, *J. Gastroenterol. Hepatol.* 27 (9) (2012) 1423–1431.
- [11] Y.F. Pan, L. Feng, X.Q. Zhang, L.J. Song, H.X. Liang, Z.Q. Li, F.B. Tao, Role of long non-coding RNAs in gene regulation and oncogenesis, *Chin. Med. J.* 124 (15) (2011) 2378–2383.
- [12] J.L. Rinn, H.Y. Chang, Genome regulation by long noncoding RNAs, *Annu. Rev. Biochem.* 81 (2012) 145–166.
- [13] T. Hung, H.Y. Chang, Long noncoding RNA in genome regulation: prospects and mechanisms, *RNA Biol.* 7 (5) (2010) 582–585.
- [14] J. Brennecke, D.R. Hipfner, A. Stark, R.B. Russell, S.M. Cohen, Bantam encodes a developmentally regulated microRNA that controls cell proliferation and regulates the proapoptotic gene *hid* in *Drosophila*, *Cell* 113 (1) (2003) 25–36.
- [15] A. Cimmino, G.A. Calin, M. Fabbri, M.V. Iorio, M. Ferracin, M. Shimizu, S.E. Wojcik, R.I. Aqeilan, S. Zupo, M. Dono, L. Rassenti, H. Alder, S. Volinia, C.G. Liu, T.J. Kippas, M. Negrini, C.M. Croce, miR-15 and miR-16 induce apoptosis by targeting BCL2, *Proc. Natl. Acad. Sci. USA* 102 (39) (2005) 13944–13949.
- [16] M.V. Iorio, M. Ferracin, C.G. Liu, A. Veronese, R. Spizzo, S. Sabbioni, E. Magri, M. Pedriali, M. Fabbri, M. Campiglio, S. Menard, J.P. Palazzo, A. Rosenberg, P. Musiani, S. Volinia, I. Nenci, G.A. Calin, P. Querzoli, M. Negrini, C.M. Croce, MicroRNA gene expression deregulation in human breast cancer, *Cancer Res.* 65 (16) (2005) 7065–7070.
- [17] H. Dong, L. Ding, F. Yan, H. Ji, H. Ju, The use of polyethylenimine-grafted graphene nanoribbon for cellular delivery of locked nucleic acid modified molecular beacon for recognition of microRNA, *Biomaterials* 32 (15) (2011) 3875–3882.
- [18] M.B. Baker, G. Bao, C.D. Searles, *In vitro* quantification of specific microRNA using molecular beacons, *Nucl. Acids Res.* 40 (2) (2012) e13.
- [19] W.J. Kang, Y.L. Cho, J.R. Chae, J.D. Lee, K.J. Choi, S. Kim, Molecular beacon-based bioimaging of multiple microRNAs during myogenesis, *Biomaterials* 32 (7) (2011) 1915–1922.
- [20] T. Gutschner, S. Diederichs, The hallmarks of cancer: a long non-coding RNA point of view, *RNA Biol.* 9 (6) (2012) 1076–1087.
- [21] R.B. Lanz, N.J. McKenna, S.A. Onate, U. Albrecht, J. Wong, S.Y. Tsai, M.J. Tsai, B.W. O'Malley, A steroid receptor coactivator, SRA, functions as an RNA and is present in an SRC-1 complex, *Cell* 97 (1) (1999) 17–27.
- [22] D. Khaitan, M.E. Dinger, J. Mazar, J. Crawford, M.A. Smith, J.S. Mattick, R.J. Perera, The melanoma-upregulated long noncoding RNA SPRY4-IT1 modulates apoptosis and invasion, *Cancer Res.* 71 (11) (2011) 3852–3862.
- [23] S. Chung, H. Nakagawa, M. Uemura, L. Piao, K. Ashikawa, N. Hosono, R. Takata, S. Akamatsu, T. Kawaguchi, T. Morizono, T. Tsunoda, Y. Daigo, K. Matsuda, N. Kamatani, Y. Nakamura, M. Kubo, Association of a novel long non-coding RNA in 8q24 with prostate cancer susceptibility, *Cancer Sci.* 102 (1) (2011) 245–252.
- [24] L. Pibouin, J. Villaudy, D. Ferbus, M. Muleris, M.T. Prosperi, Y. Remvikos, G. Goubin, Cloning of the mRNA of overexpression in colon carcinoma-1: a sequence overexpressed in a subset of colon carcinomas, *Cancer Genet. Cytogenet.* 133 (1) (2002) 55–60.
- [25] R.A. Gupta, N. Shah, K.C. Wang, J. Kim, H.M. Horlings, D.J. Wong, M.C. Tsai, T. Hung, P. Argani, J.L. Rinn, Y. Wang, P. Brzoska, B. Kong, R. Li, R.B. West, M.J. van de Vijver, S. Sukumar, H.Y. Chang, Long non-coding RNA HOTAIR reprograms chromatin state to promote cancer metastasis, *Nature* 464 (7291) (2010) 1071–1076.
- [26] Z. Yang, L. Zhou, L.M. Wu, M.C. Lai, H.Y. Xie, F. Zhang, S.S. Zheng, Overexpression of long non-coding RNA HOTAIR predicts tumor recurrence in hepatocellular carcinoma patients following liver transplantation, *Ann. Surg. Oncol.* 18 (5) (2011) 1243–1250.
- [27] E. Pasmant, I. Laurendeau, D. Heron, M. Vidaud, D. Vidaud, I. Bieche, Characterization of a germ-line deletion, including the entire INK4/ARF locus, in a melanoma-neural system tumor family: identification of ANRIL, an antisense noncoding RNA whose expression coclusters with ARF, *Cancer Res.* 67 (8) (2007) 3963–3969.
- [28] P. Ji, S. Diederichs, W. Wang, S. Boing, R. Metzger, P.M. Schneider, N. Tidow, B. Brandt, H. Buerger, E. Bulk, M.O. Thomas, W.E. Berdel, H. Serve, C. Muller-Tidow, MALAT-1, a novel noncoding RNA, and thymosin beta4 predict metastasis and survival in early-stage non-small cell lung cancer, *Oncogene* 22 (39) (2003) 8031–8041.
- [29] V. Tanos, D. Prus, S. Ayesh, D. Weinstein, M.L. Tykocinski, N. De-Groot, A. Hochberg, I. Ariel, Expression of the imprinted H19 oncofetal RNA in epithelial ovarian cancer, *Eur. J. Obstet. Gynecol. Reprod. Biol.* 85 (1) (1999) 7–11.
- [30] A. Nissan, A. Stojadinovic, S. Mitran-Rosenbaum, D. Halle, R. Grinbaum, M. Roistacher, A. Bochem, B.E. Dayanc, G. Ritter, I. Gomceli, E.B. Bostanci, M. Akoglu, Y.T. Chen, L.J. Old, A.O. Gure, Colon cancer associated transcript-1: a novel RNA expressed in malignant and pre-malignant human tissues, *Int. J. Cancer* 130 (7) (2012) 1598–1606.
- [31] Y. Kam, A. Rubinstein, A. Nissan, D. Halle, E. Yavin, Detection of endogenous K-ras mRNA in living cells at a single base resolution by a PNA molecular beacon, *Mol. Pharm.* 9 (3) (2012) 685–693.
- [32] S. Tyagi, Imaging intracellular RNA distribution and dynamics in living cells, *Nat. Methods* 6 (5) (2009) 331–338.
- [33] S. Kummer, A. Knoll, E. Socher, L. Bethge, A. Herrmann, O. Seitz, PNA FIT-probes for the dual color imaging of two viral mRNA targets in influenza H1N1 infected live cells, *Bioconjugate Chem.* 23 (10) (2012) 2051–2060.
- [34] S. Kummer, A. Knoll, E. Socher, L. Bethge, A. Herrmann, O. Seitz, Fluorescence imaging of influenza H1N1 mRNA in living infected cells using single-chromophore FIT-PNA, *Angew. Chem. Int. Ed.* 50 (8) (2012) 1931–1934.
- [35] L. Bethge, D.V. Jarikote, O. Seitz, New cyanine dyes as base surrogates in PNA: forced intercalation probes (FIT-probes) for homogeneous SNP detection, *Bioorg. Med. Chem.* 16 (1) (2008) 114–125.
- [36] O. Kohler, D.V. Jarikote, O. Seitz, Forced intercalation probes (FIT probes): thiazole orange as a fluorescent base in peptide nucleic acids for homogeneous single-nucleotide-polymorphism detection, *ChemBioChem* 6 (1) (2005) 69–77.
- [37] M. Zuker, Mfold web server for nucleic acid folding and hybridization prediction, *Nucl. Acids Res.* 31 (13) (2003) 3406–3415.
- [38] P.E. Nielsen, PNA technology, *Methods Mol. Biol.* 208 (2002) 3–26.
- [39] D.V. Jarikote, O. Kohler, E. Socher, O. Seitz, Divergent and linear solid-phase synthesis of PNA containing thiazole orange as artificial base, *Eur. J. Org. Chem.* 15 (2005) 3187–3195.
- [40] J.C. Kim, S.A. Roh, K.H. Koo, Y.K. Cho, H.C. Kim, C.S. Yu, S.J. Oh, J.S. Ryu, D.C. Bicknell, W.F. Bodmer, Preclinical application of radioimmunoguided surgery using anti-carcinoembryonic antigen biparatopic antibody in the colon cancer, *Eur. Surg. Res.* 37 (1) (2005) 36–44.
- [41] D.M. Agnese, S.F. Abdessalam, W.E. Burak Jr., M.W. Arnold, D. Soble, G.H. Hinkle, D. Young, M.B. Khazaeli, E.W. Martin Jr., Pilot study using a humanized CC49 monoclonal antibody (HuCC49DeltaCH2) to localize recurrent colorectal carcinoma, *Ann. Surg. Oncol.* 11 (2) (2004) 197–202.
- [42] S. Schneebaum, E. Even-Sapir, M. Cohen, H. Shacham-Lehrman, A. Gat, E. Brazovsky, G. Livshitz, J. Stadler, Y. Skornick, Clinical applications of gamma-detection probes – radioguided surgery, *Eur. J. Nucl. Med.* 26 (4 Suppl.) (1999) S26–S35.
- [43] A. Muxi, F. Pons, S. Vidal-Sicart, F.J. Setoain, R. Herranz, F. Novell, R.M. Fernandez, M. Trias, J. Setoain, Radioimmunoguided surgery of colorectal carcinoma with an <sup>111</sup>In-labelled anti-TAG72 monoclonal antibody, *Nucl. Med. Commun.* 20 (2) (1999) 123–130.
- [44] T. Shiraiishi, P.E. Nielsen, Enhanced cellular delivery of cell-penetrating peptide-peptide nucleic acid conjugates by photochemical internalization, *Methods Mol. Biol.* 683 (2011) 391–397.
- [45] A.G. Torres, M.M. Fabiani, E. Vigorito, D. Williams, N. Al-Abaidi, F. Wojciechowski, R.H. Hudson, O. Seitz, M.J. Gait, Chemical structure requirements and cellular targeting of microRNA-122 by peptide nucleic acids anti-miRs, *Nucl. Acids Res.* 40 (5) (2012) 2152–2167.
- [46] T. Hagiwara, J. Hattori, T. Kaneda, PNA-*in situ* hybridization method for detection of HIV-1 DNA in virus-infected cells and subsequent detection of cellular and viral proteins, *Methods Mol. Biol.* 326 (2006) 139–149.
- [47] A.M. Blanco, R. Artero, A practical approach to FRET-based PNA fluorescence *in situ* hybridization, *Methods* 52 (4) (2010) 343–351.